

Initial Test Experiments with a Beamformer at the Allen Telescope Array

Robert Ackermann

June 30, 2005

An inexpensive, modest (up to 8 antennas single pol. or 4 antennas dual pol.) beamformer has been developed as a tool to facilitate software development and testing towards the eventual IFP implementation. The beamformer is specifically designed to attach to the baseband outputs of the RPA downconverter. It was recently brought to Hat Creek for the first time to undergo tests to verify its performance off of the bench. There was also some hope an internal numerically controlled oscillator and mixer added to one of its output stages could be used to smoothly remove Doppler from the planned, but sadly not possible, 2250.0 MHz COSMOS-1 solar sail observations.



Figure 1: beamformer assembled in 4U server rack-mount case

The beamformer is meant to play a similar role in the development of IFP control software as A0 did for the development of antenna control software and the software correlator did for early evaluation of feed performance and dish surfaces. Considering that, the beamformer is implemented using the IFP 'T' architecture. Although planned independently and before knowledge of the NSF grant opportunity, a strong but failed effort was made to ready the beamformer in time for possible use towards achieving NSF proposal results.

A picture of the assembled beamformer (Figure 1) shows a standard mini-ITX motherboard (bluish board middle-left) along with its associated power supply and disk drives (top-left and top-right), the beamformer board (green board bottom-right) under control of the motherboard through the secondary IDE interface, and a baseband to NSS upconverter (brownish board bottom-left). All circuitry obtains voltage from the computer ATX power supply.

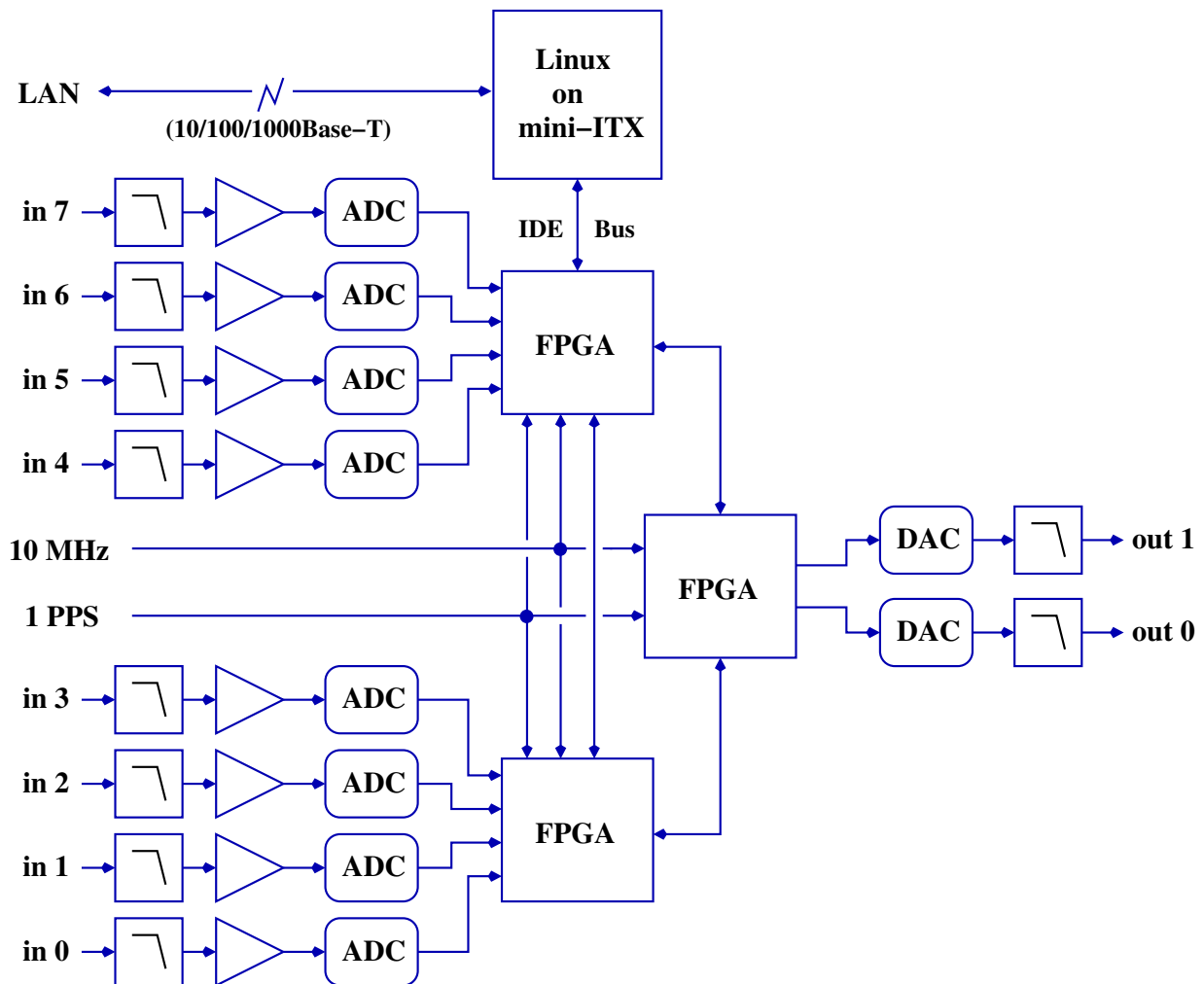


Figure 2: beamformer board hardware block diagram (upconverter not shown)

The beamformer board hardware block diagram (Figure 2) illustrates the central FPGA-based processing architecture which includes 8 channels of analog input and 2 channels of analog output. Currently, only 4 channels of analog input are populated (4, 5, 6, and 7), which matches with one pole each of PTA antennas 1, 2, 3, and 4. It is anticipated the dual output channels could be useful for early, limited (by array element number) nulling and signal classification (in main beam or side-lobes?) experiments. There are wide signal paths between each FPGA pair and between the top FPGA and the mini-ITX motherboard. The interconnectivity and selected speed and size characteristics of the FPGAs exceed what is necessary for the beamformer application. This was done with consideration of two potential other applications of the "beamformer" hardware:

- add baselines in conjunction with the existing FX4 correlator
- provide a filament from a synthesized beam to Fugue or an early SonATA prototype (the filament would flow from the top FPGA, through the IDE Bus, and then through the mini-ITX LAN port)

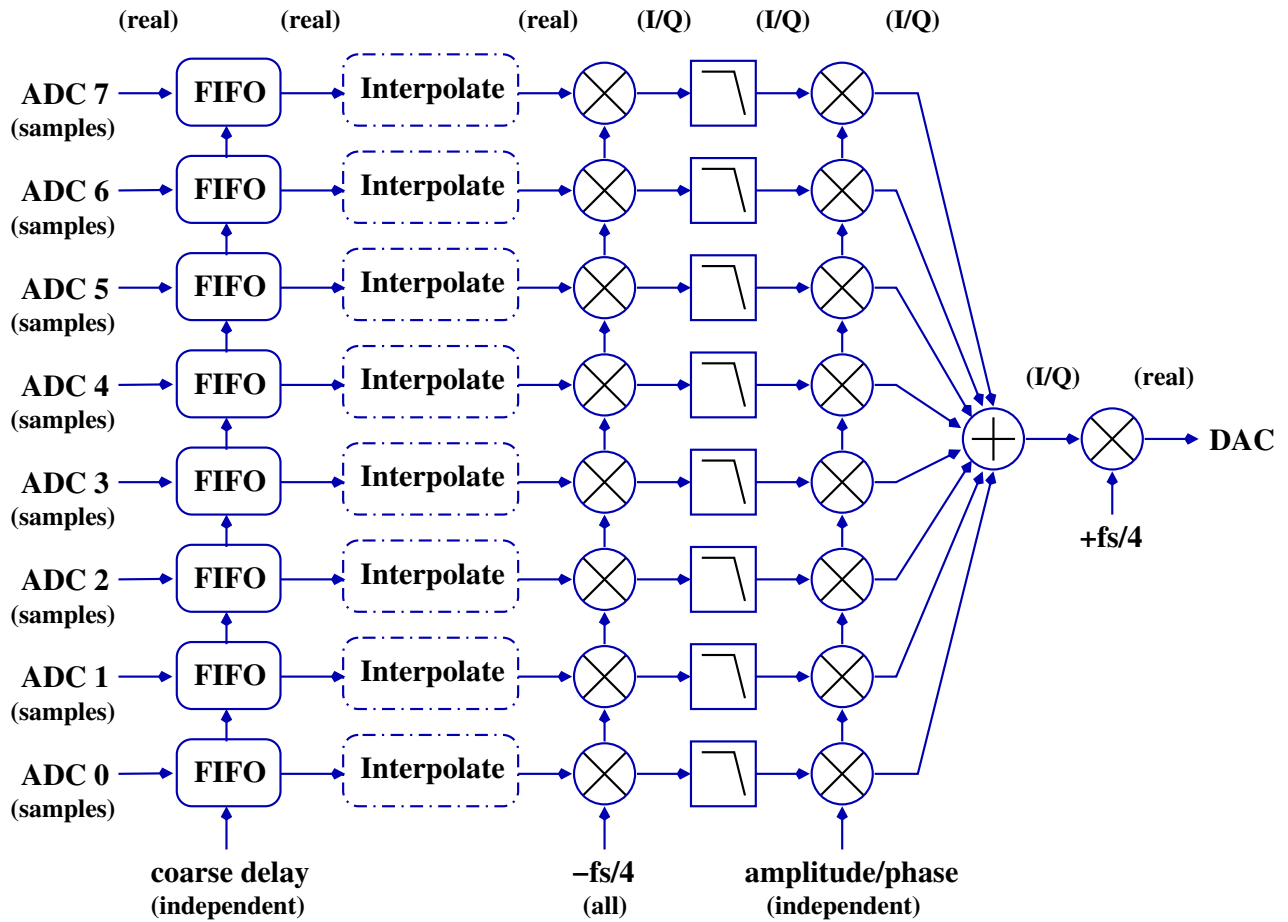


Figure 3: beamformer combined code block diagram (for one output channel)

The beamformer code block diagram (Figure 3) illustrates the functional result of the combined code from all three FPGAs for a single output channel (of two). Each input ADC 8-bit sample stream feeds a FIFO that is maintained half-full when the delay is set to zero nanoseconds. This allows each input channel to be set for negative, zero, or positive delay. The FIFOs are sized by FPGA code to be conservatively larger than twice the worst case baseline plus cable delays (in samples) over the antenna pairs. Fine sub-sample interpolation delay is not currently implemented (indicated by dashed boxes). Instead, fine delay is set for the middle of the band using later-stage phase rotation with understood and accepted chromatic aberration increasing towards the band edges. After the delay operation, each real sample stream is mixed down to complex baseband and then multiplied by an independent phasor before summation. The summed (combined) stream is then mixed back up from complex baseband upon which the real part is selected to drive a 14-bit DAC. Currently, the ADC anti-alias filters and DAC output filters are selected for 50MHz Nyquist sampling, which works (because of the anti-alias filters) with either the modified or the unmodified RFA downconverter channels. The sample rate is established by PLLs in the FPGAs which lock to the site 10MHz reference.

The utility of the baseband to NSS upconverter board associated with the beamformer is in question given recent progress towards converting the inputs of Prelude to baseband to accommodate the DAC analog outputs of the IFP. Nevertheless, a short experiment was conducted to verify the operation of the upconverter. The upconverter is active and based on a slight misapplication of a basic cellular phone mixer chip. The test signal for this experiment and subsequent delay experiments in this paper was selected from a portion of the Solidaridad-2 satellite spectrum. Solidaridad-2 was chosen for these initial

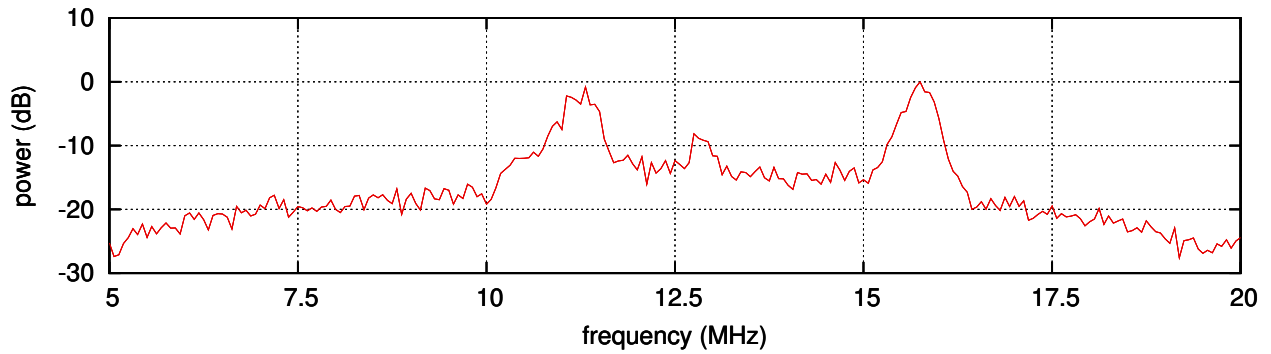


Figure 4: Solidaridad-2 spectrum measured at upconverter IF input

experiments because of its identifiable spectral features, good S/N, reasonably stable power, and geostationary orbit (so that antenna phase relationships remain stable). Three peaks from the Solidaridad-2 spectrum (Figure 4) are shown roughly centered in the upconverter IF input. Those same peaks are shown mirrored (Figure 5) around the central LO in the negative and positive mixing bands of the upconverter RF output. Note that the LO was tuned to 1050 MHz which is almost double the nominal center frequency of the NSS. This was due to the fact that the only free LO available (the LO associated with the SETI downconverter) would not tune below 1 GHz. Fortunately, the higher LO frequency used in this experiment was still marginally within the operating range of the active mixer. For this experiment and all other experiments described in this paper, the detector (measurement tool) used was a HP spectrum analyzer. The spectrum analyzer was selected for its frequency range and to minimize experimental variables. Future experiments that use the beamformer baseband analog outputs will likely feed autocorrelation channels of the FX4 correlator.

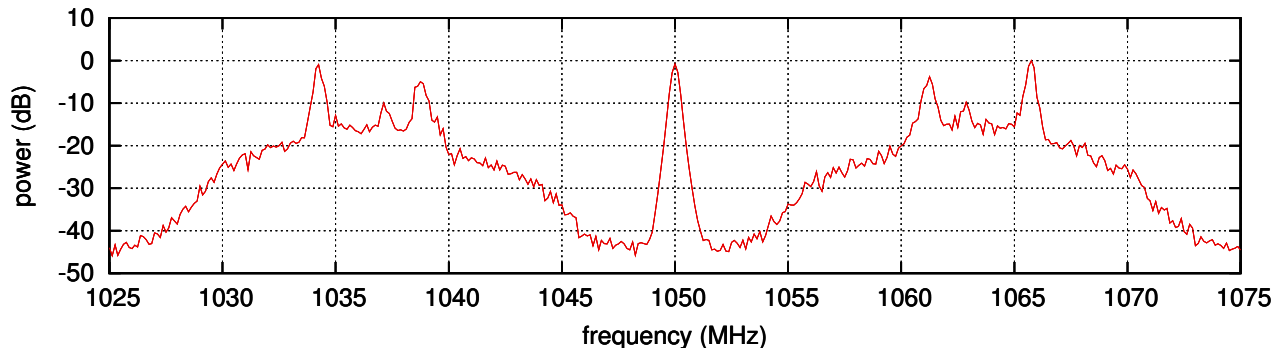


Figure 5: Solidaridad-2 spectrum measured in upconverter RF output bands

The most significant experiment accomplished so far to verify the internal functions of the beamformer was to slide one polarization of antennas 1, 3, and 4 in time (nanoseconds) with respect to one polarization of antenna 2 searching for optimum delay. Antenna 2 was chosen as the reference so that the delay settings found with the beamformer could be compared to the fixed delays already determined with the FX4 correlator, which also assigns antenna 2 as its reference (i.e., 0 ns delay). The experiment began with the intention of searching for the peak of a sync function generated by plotting total summed power versus relative delay for each antenna pair while detecting a wide-band source. Unfortunately, this was thwarted by the current lack of baseline and signal path calibration needed to perform fringe stopping on a celestial source and recent hardware additions and maintenance which resulted in lack of confidence of the state of polarization orientation between antenna channels. The "white light" signal desirable for

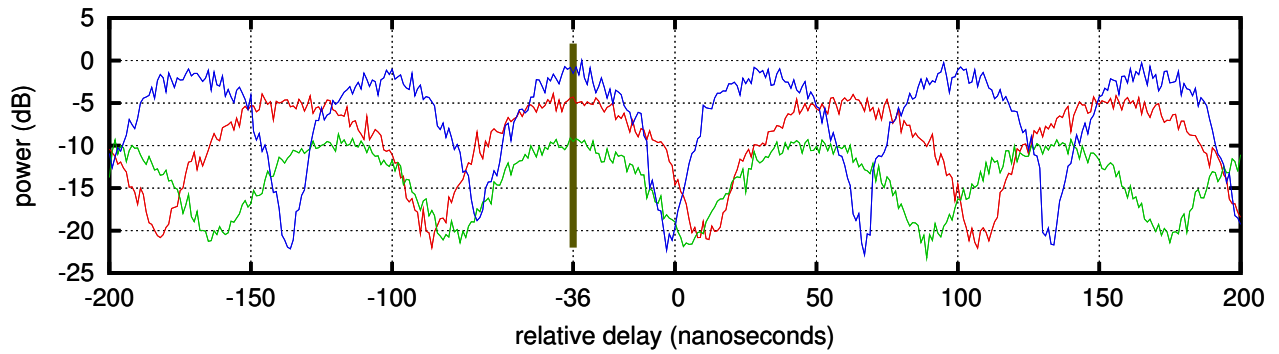


Figure 6: Antenna 3 delay with respect to Antenna 2 (one pol. channel each)

this experiment was grossly approximated by selecting three high S/N separated baseband frequencies (10.4 MHz, 11.9 MHz, and 14.7 MHz): one from each peak of the three grouped features found in the Solidaridad-2 spectrum. The circular polarization of the Solidaridad-2 signal protected against possible orthogonal polarization pairs, resulting in small delay offsets, in that event, instead of experimental failure. Power measured for each of the three selected frequencies versus delay for antenna 3 with respect

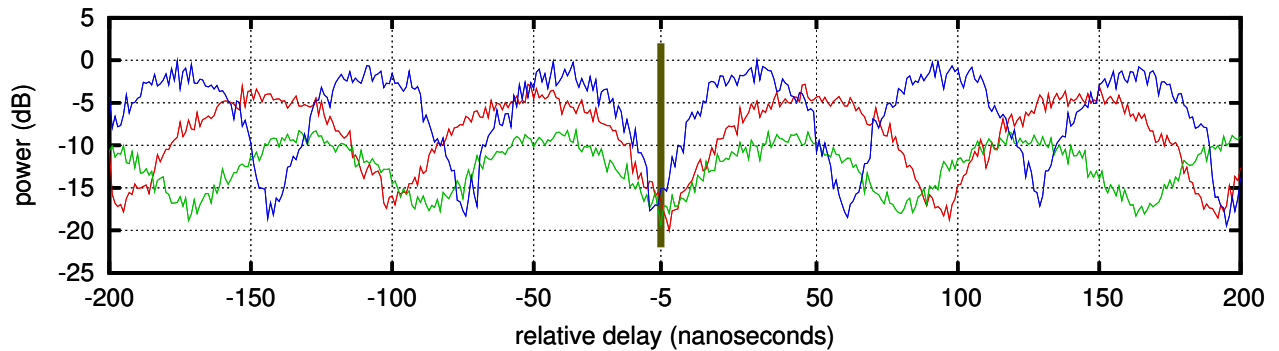


Figure 7: Antenna 1 delay with respect to Antenna 2 (one pol. channel each)

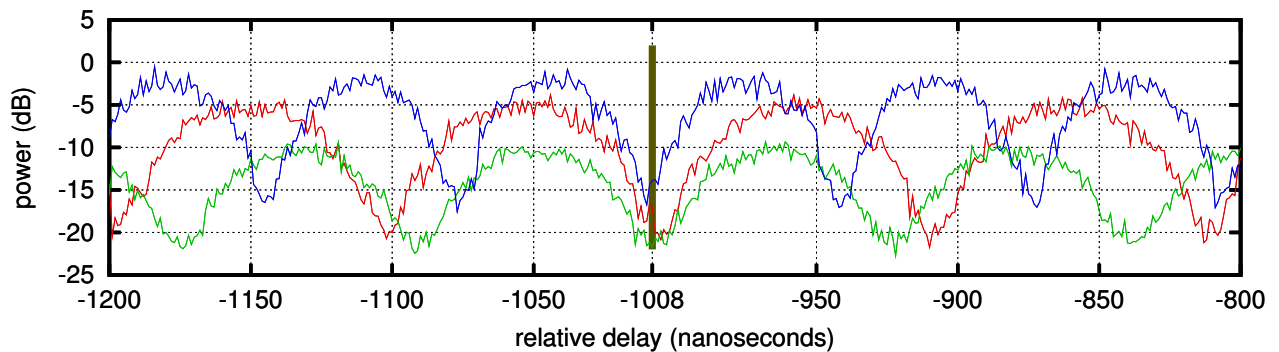


Figure 8: Antenna 4 delay with respect to Antenna 2 (one pol. channel each)

to antenna 2 (Figure 6) shows a simultaneous peak in power for all three frequencies at -36 nanoseconds; however, the simultaneous peaks were fortuitous because the array currently lacks calibration to predict phase and phase space was not searched, other than the quarter turn of phase rotation used to set fine delay. Power measured for the same three frequencies versus delay for antenna 1 with respect to antenna 2 (Figure 7) and antenna 4 with respect to antenna 2 (Figure 8) shows a coincidental effect on power and a symmetry (i.e., the place where there would be peaks with proper phase settings) at -5 and

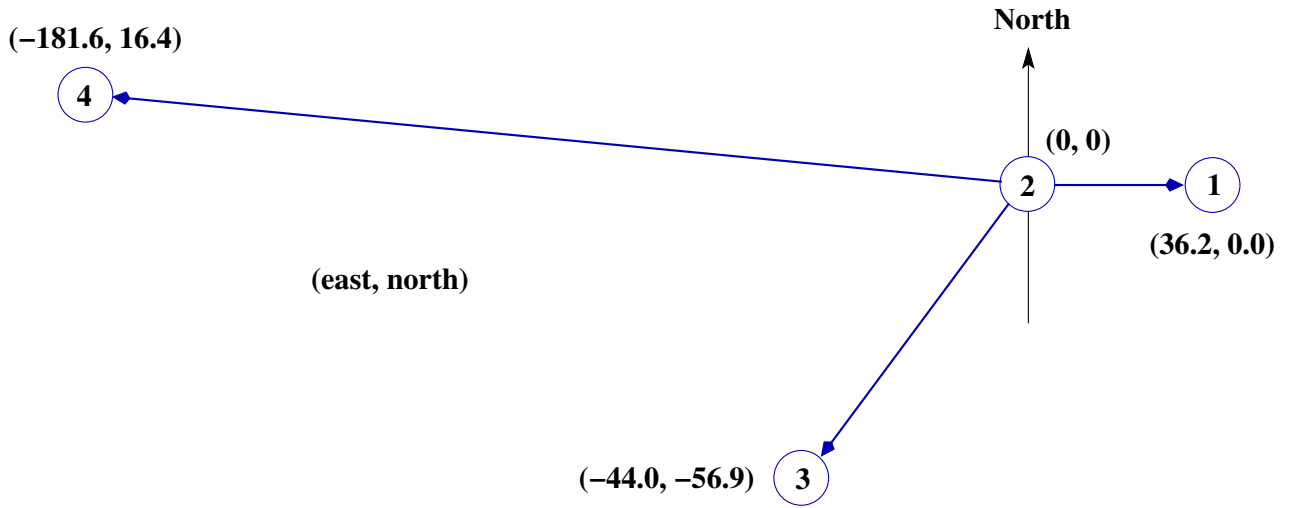


Figure 9: baseline vectors for antennas 1, 3, and 4 (excluding height) in nanoseconds

-1008 nanoseconds respectively. Note that the search window for antenna four (Figure 8) was offset to a large negative delay. This was done with prior knowledge of the FX4 correlator fixed delays and with the author’s personal experience having been on the team that pulled the optical fiber for antenna four along the much longer southern route to the control building; however, an alternative delay point not distinguishable from the delay point chosen (possibly an inverse bandwidth periodic feature) was found in the data at -332 nanoseconds (not within the range of the Figure 8 graph).

Table 1: beamformer delay values compared with FX4 correlator fixed values

Antenna	Experimental (ns)	Geometric (ns)	Beamformer Fixed (ns)	FX4 Fixed (ns)
1	-5	6	-11	-18
3	-36	34	-70	-77
4	-1008	-42	-966	-990

Optimum delay values determined with the beamformer as described in the above experiments must have geometric delay subtracted to compare with the fixed (“bulk” or zenith) delays of the FX4 correlator. Geometric delay was computed from the inner product of the antenna baseline vectors in nanoseconds (Figure 9) with the normalized Cartesian pointing vector converted from the Solidaridad-2 polar azimuth and elevation coordinates (167.0, 42.1). The antenna locations are currently known to the accuracy and precision of GPS survey with probable small pedestal offsets during construction. Comparison of the beamformer experimentally determined fixed delays with the FX4 correlator fixed delays (Table 1) reveal reasonable differences considering various accepted tolerances and the current environment, upon which we are improving, where polarization swapping can occur and fiber and coax patch cable length mismatches are not always carefully considered. It is interesting; however, that the beamformer fixed delay values are larger (more positive) in all three antenna cases than the FX4 correlator fixed delay values.

Results from these initial experiments provide guarded confidence in the proper operation of the core functionality of the beamformer. Future goals include mapping a synthesized beam and tracking a celestial object with a synthesized beam.